

# Aeroelastic Balance

Yin Zhou, M.ASCE,<sup>1</sup> and Ahsan Kareem, M.ASCE<sup>2</sup>

**Abstract:** The “stick” type aeroelastic model, referred to here as “aeroelastic balance,” has served as an effective tool for investigating wind-induced response of tall buildings and towers in both fundamental research as well as design applications. However, some questions still remain unaddressed in the available literature regarding the efficacy of the aeroelastic balance as a design tool. These concerns arise from the mismatch of the mode shape and mass distribution between the model and the prototype. This paper provides appropriate scaling laws needed for modeling building dynamics and aeroelastic effects and offers a critical evaluation of the modeling issues concerning the aeroelastic balance. Clearly, buildings with a nonlinear mode shape preclude a straightforward similarity between the model and the prototype displacement and acceleration response. Similar concerns come to light from a mismatch in the mass distribution when the aeroelastic effects are present. In this paper, procedures based on the base bending moment of the aeroelastic balance are developed for scaling model test data for predicting the prototype structural response. Currently used aeroelastic modeling practices are critically reviewed in light of this scheme. The proposed procedures capture the dynamics of wind–structure interactions without the shortcomings of current practices.

**DOI:** 10.1061/(ASCE)0733-9399(2003)129:3(283)

**CE Database keywords:** Wind loads; Wind tunnels; Buildings, high-rise; Aeroelasticity; Aerodynamics; Turbulence.

## Introduction

The analytical modeling of wind–structure interactions is mathematically impracticable; therefore, wind tunnels have served as the most reliable means of investigating wind load effects on structures. Although recent advances in computational fluid dynamics are very promising, these are not at a stage of becoming a designer’s tool in the near future. Among several existing wind tunnel modeling approaches, the “stick” type aeroelastic model and the “high frequency base balance” (HFBB) technique are not only the most popular, but also very efficient. The stick model has the extra advantage over the HFBB test that it can include the contribution of aeroelastic effects, which may become essential for certain wind sensitive structures. In comparison with other aeroelastic models, i.e., the “multidegree-of-freedom aeroelastic model,” the stick type model is more efficient in terms of design, fabrication, calibration, and measurements, which presents savings in both time and cost. Furthermore, this test also allows convenient changes in the mass, stiffness, and damping and even geometric properties. In light of these attributes, the stick type aeroelastic model test has played a profoundly significant and

sometimes irreplaceable role in both structural design and basic research concerning tall buildings and towers since the development of boundary layer wind tunnel facilities.

For the wind-induced response of most tall structures, only the response in the fundamental modes has been noted to be significant (Kareem 1982). This feature favors a simplified stick type model test in which two fundamental translation modes are simulated. A typical set up of the stick type aeroelastic model is schematically shown in Figs. 1(a and c). Variations of this configuration have been reported by Whitebread and Scruton (1965); Kareem and Cermak (1979); Isyumov (1982); Saunders and Melbourne (1975); Boggs (1991), and others. The model in Fig. 1(c) also includes a provision for modeling the torsional degree of freedom, but it only represents a uniform mode shape. Therefore, the torsional response requires a mode shape correction. A typical stick model involves the building shell configuration, spring, mass, and damping devices. The modeling of mass, stiffness and damping, geometric shape, and approach flow environment has been recognized to be critical for this kind of model. The displacement or acceleration at the top or at another height and/or the base bending moment (BBM) about the axis of rotation are measured. The stick aeroelastic model test is important in assessing both the aeroelastic and dynamic response of structures under winds. The aeroelastic effects of interest range from the potential of aeroelastic instability to situations where negative aerodynamic damping results in significant response magnification. An accurate modeling of both the structural dynamic response and the contribution of aeroelastic effects is extremely important for wind sensitive structures.

This paper focuses on the relevant features concerning the role of a stick type aeroelastic model in structural design. Unlike the HFBB test, the stick aeroelastic model test provides a “direct” estimation of the wind-induced response. Therefore, a direct similarity between the model and the prototype structure is a prerequisite for accurate assessment of wind effects. However, this cannot always be easily achieved in practice. The first issue concerns

<sup>1</sup>Research Associate, Dept. of Civil Engineering and Geological Sciences, Univ. of Notre Dame, Notre Dame, IN 46556. E-mail: yzhou@nd.edu

<sup>2</sup>Robert M. Moran Professor, Dept. of Civil Engineering and Geological Sciences, Univ. of Notre Dame, Notre Dame, IN 46556. E-mail: kareem@nd.edu

Note. Associate Editor: Laurence J. Jacobs. Discussion open until August 1, 2003. Separate discussions must be submitted for individual papers. To extend the closing date by one month, a written request must be filed with the ASCE Managing Editor. The manuscript for this paper was submitted for review and possible publication on July 30, 2001; approved on May 1, 2002. This paper is part of the *Journal of Engineering Mechanics*, Vol. 129, No. 3, March 1, 2003. ©ASCE, ISSN 0733-9399/2003/3-283–292/\$18.00.

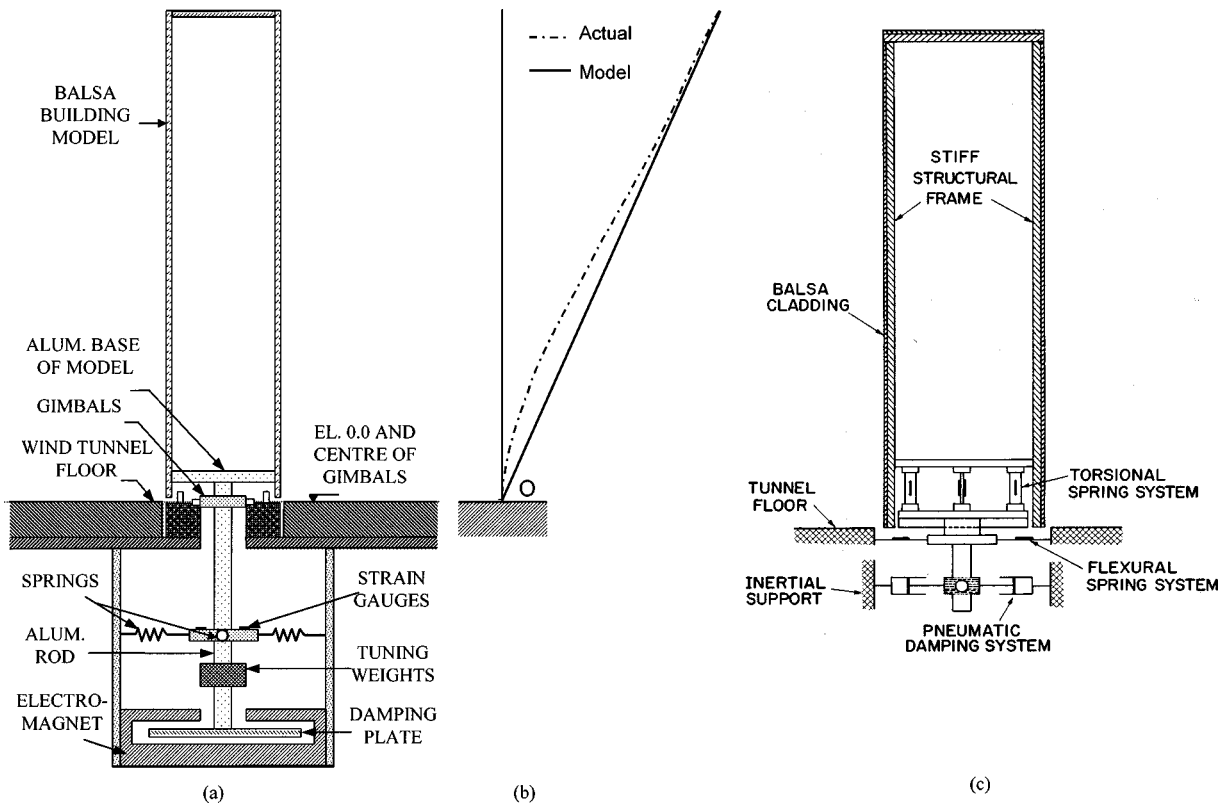


Fig. 1. Aeroelastic balance: (a) base-pivoted model; (b) mode shape modeling; (c) base-spring model

the mode shape modeling because this type of test works best for structures with a linear first mode shape [Fig. 1(b)]. However many tall buildings, especially tall, flexible, and slender buildings, have mode shapes that may deviate from a straight line [Fig. 2(a)]. The second issue of concern arises from the modeling of mass. Tall buildings usually have a complex mass distribution [Fig. 2(b)], which poses a difficulty in replicating it in a small-scale aeroelastic model.

The inconsistency resulting from the mismatch in mode shape modeling has been generally treated in two ways. One approach utilizes a straight-line mode shape to “fit” a large portion of the actual mode shape through adjustment of the pivot point at an “appropriate” height above the building base (Isyumov 1982). Alternatively, analytical procedures may be invoked to adjust the model test observations for nonlinear mode shapes (e.g., Vickery 1970; Kareem 1984; Vickery et al. 1985; Holmes 1987; Boggs 1991; Xu et al. 1993; Kijewski and Kareem 1998; Zhou et al. 1999, 2002). Most of the analytical corrections follow the techniques routinely used in the HFBB; their effectiveness in this context needs further examination.

The effect of imperfect modeling of the mass distribution has received relatively less attention. Significant variations concerning the mass modeling have been noted in the literature. For example, in some of the literature (e.g., Cermak 1977; Isyumov 1982; and ASCE 1999) the similarities in the total and the first-mode generalized masses, and the mass moment of inertia (MMI) are required; while in others the exact modeling of mass has been relaxed (e.g., Bienkiewicz et al. 1986; and Boggs 1991).

In this paper, first scaling laws for the model design are derived. The effect of imperfect modeling of mass is delineated through a comparison of the model with a prototype building having a linear mode shape. This is followed by highlighting the effect of nonlinear mode shape on the response predictions based

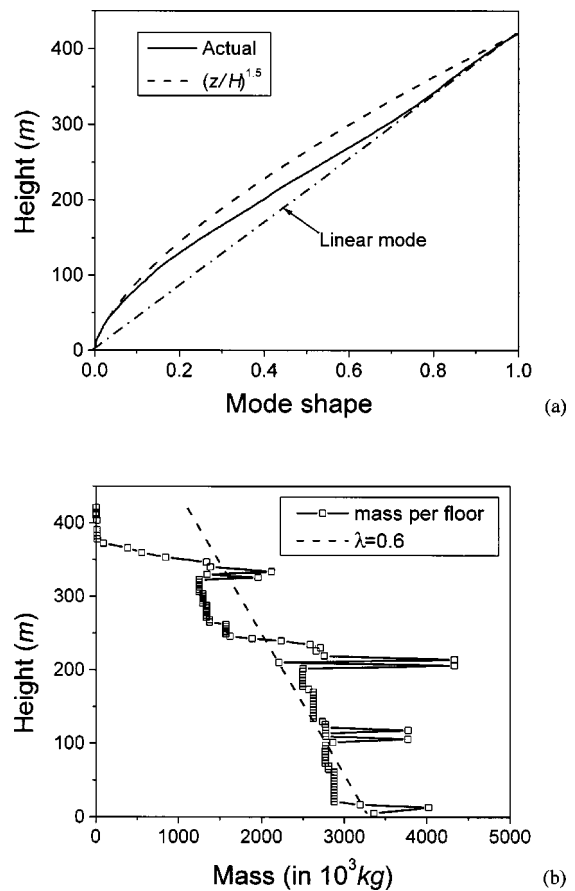


Fig. 2. Example of actual high-rise building (Gu et al. 1999): (a) mode shape; (b) mass distribution

on a linear mode shape as implied in the stick type aeroelastic test. Based on a previous study related to the effects of nonlinear mode shapes on structural response (Zhou et al. 2002), analytical procedures are developed to determine the equivalent static wind load (ESWL) and associated wind-induced response of prototype buildings with arbitrary mode shapes by utilizing the BBM measurements. The efficacy of two currently used aeroelastic modeling practices is also assessed in light of the schemes presented here.

### Dynamic Similitude: Linear Mode Shape

Scaling laws that describe the relationship between the scaled model and the prototype building involving linear mode shape are derived. Although the similarity between the model and the prototype is generally well understood, this paper highlights some features that may result in the introduction of improper scaling.

Scaling laws can be obtained either by a dimensional analysis or by nondimensional equations of motion (Langhaar 1951). The latter approach is used here since for the stick type aeroelastic models the response in fundamental modes dominates the overall response. Without loss of generality, the equation of motion governing the motion of a tall structure with an arbitrary mode shape is given below

$$m^* \ddot{\xi}(t) + c^* \dot{\xi}(t) + k^* \xi(t) = P^*(t, \xi, \dot{\xi}, \ddot{\xi}, \dots) \quad (1)$$

where  $m^* = \int_0^H m(z) \varphi^2(z) dz$ ,  $c^* = 2\zeta \sqrt{k^* m^*}$ ,  $k^* = (2\pi f_1)^2 m^*$ ,  $P^* = \int_0^H P(z, t) \varphi(z) dz$ ; and  $\xi$ =generalized mass, damping, stiffness, wind force, and displacement in the first mode, respectively;  $\zeta$ =structural critical damping ratio;  $f_1$ =first mode natural frequency; the motion dependent terms that appear in the right hand side of Eq. (1) represent the feedback due to aeroelastic effects; and  $P(z, t)$ =externally applied wind load. The mode shape of an actual building can usually be well approximated by a power-law expression  $\varphi(z) = c(z/H)^\beta$ , in which  $c$ =normalization factor and  $\beta$ =exponent of the mode shape, which is unity for a linear mode shape. In order to avoid arbitrariness in the normalization invoked in the generalized equation of motion, scaling laws are derived based on the displacement at the building top. Recasting Eq. (1) accordingly

$$\ddot{Y}_H(t) + 4\pi f_1 \zeta \dot{Y}_H(t) + (2\pi f_1)^2 Y_H(t) = \frac{1}{\mathbf{m}} \int_0^H P(z, t, Y, \dot{Y}, \ddot{Y} \dots) \cdot (z/H)^\beta dz \quad (2)$$

where  $Y_H = c \cdot \xi$ =displacement at the building top,  $H$ ; and  $\mathbf{m} = \int_0^H m(z) \cdot (z/H)^{2\beta} dz$ =first mode generalized mass (MGM) or first MGM. It is noted that the first MGM is a special case of the generalized mass  $m^*$ , in which the normalization factor  $c$  is equal to unity.

For a building with linear mode shapes, Eq. (2) can be simplified as

$$\ddot{Y}'_H(t) + 4\pi f_1 \zeta \dot{Y}'_H(t) + (2\pi f_1)^2 Y'_H(t) = \frac{M(t, Y', \dot{Y}', \ddot{Y}' \dots)/H}{\mathbf{m}'} \quad (3)$$

where the superscript prime denotes quantities based on the linear mode shape; while  $\mathbf{m}' = \int_0^H m(z) \cdot (z/H)^2 dz = I/H^2$ , in which  $I$ =MMI; and  $M = \int_0^H P(z, t) \cdot z dz$ =BBM due to the externally applied wind pressures, which can be expressed as

$$M(t, Y', \dot{Y}', \ddot{Y}' \dots) = C_M(t, Y', \dot{Y}', \ddot{Y}' \dots) \cdot (1/2\rho_a \bar{V}_H^2 \sqrt{BDH^2}) \quad (4)$$

where  $C_M$ =dimensionless BBM coefficient;  $\rho_a$ =air density;  $\bar{V}_H$ =mean reference wind velocity at the building top; and  $B$  and  $D$ =width and depth of the building, respectively. It is noteworthy that Eq. (4) is only comprised of quantities that have physical meaning. Based on this equation, a detailed derivation of scaling laws for a prototype building with linear mode shape is provided in Appendix I.

The scaling law given in Eq. (37) concerns the first MGM. When the mass distribution of the model follows exactly that of the prototype, the similarity requirement in Eq. (37) is equivalent to that of the total mass

$$(K_{m_T}/K_L^3) \cdot (1/K_{\rho_a}) = 1 \quad (5)$$

or

$$(\rho_s/\rho_a)_m = (\rho_s/\rho_a)_p \quad (6)$$

where the subscript  $m$  represents the model and  $p$  the prototype;  $\mathbf{m}_T = \int_0^H m(z) dz$ =total mass of the building; and  $\rho_s$ =structural bulk density. Eq. (6) has been documented in most of the literature (e.g., Cermak 1977; Kareem and Cermak 1978; ASCE 1999) as the requirement for maintaining a constant ratio between the structural bulk density and the air density. For linear mode shapes, using the relationship between the first MGM and the MMI, the following relationship is obtained:

$$I_m = K_L^5 \cdot K_{\rho_a} \cdot I_p \quad (7)$$

which has been referred to as the similarity requirement for the MMI in the literature (e.g., Isyumov 1982; Boggs 1991).

Since the model has the same mode shape as the prototype in this particular case, fulfillment of any one of the three scaling requirements in Eqs. (37), (6), or (7) guarantees the remaining two, provided that the mass distribution of the prototype structure is precisely replicated in the model. This has led to the selection of one of these three relationships indiscriminately in model design. It should be emphasized that the equivalence between these relationships is contingent upon the condition of matching of the mass distribution and the linear mode shape.

Many actual buildings usually feature complicated mass distributions; one such example is shown in Fig. 2. It is very difficult to accurately reproduce this mass distribution in the aeroelastic model test at a small-scale, e.g., around 1/300–1/500.

Evidently, using the same total mass with different distributions, both the first MGM and the MMI could be significantly different. This means that the similarity of the total mass or the density ratio could not ensure correct modeling of the first MGM or the MMI because of the possible differences in the mass distribution. It is very important to note that the derivation of the scaling laws based on the dimensional analysis would not reflect this difference since both the total mass and the first MGM have the same dimensions. However, as shown in the derivation of scaling laws in Appendix I, it is the first MGM or MMI that plays the key role in the modeling of building displacement or acceleration response. This observation can also be made from the following equation for the root mean square (RMS) of the displacement response based on Eq. (3):

$$\sigma'_Y(z) = \frac{1}{(2\pi f_1)^2 \cdot \int_0^H m(z) (z/H)^2 dz} \cdot \left( \int_0^\infty |H(f)|^2 \cdot S_M(f)/H^2 \cdot df \right)^{1/2} \cdot \left( \frac{z}{H} \right) \quad (8)$$

where  $|H(f)|^2 = \{[1 - (f/f_1)^2]^2 + (2\zeta f/f_1)^2\}^{-1}$  = structural transfer function; and  $S_M(f)$  = power spectral density (PSD) of the external BBM under the wind pressures.

Eq. (8) can be used for displacement or acceleration measurement based techniques. On the other hand, although the displacement or acceleration response is important, the ESWL usually offers a more convenient means of estimating wind-induced load effects for design. Extending the displacement in Eq. (8), the ESWL in the case of dynamically sensitive structures can be represented by the inertial force

$$\sigma'_p(z) = (2\pi f_1)^2 \cdot m(z) \cdot \sigma'_Y(z) = \frac{1}{H \cdot \int_0^H m(z) (z/H)^2 dz} \cdot \left( \int_0^\infty |H(f)|^2 \cdot S_M(f) \cdot df \right)^{1/2} \cdot \left( \frac{z}{H} \right) \cdot m(z) \quad (9)$$

Accordingly, the BBM response can be computed by

$$\sigma'_M = \int_0^H \sigma'_p(z) \cdot z \, dz = \left( \int_0^\infty |H(f)|^2 \cdot S_M(f) \cdot df \right)^{1/2} \quad (10)$$

Here the subscript **P** and **M**, which use the same symbol but expressed in bold, represent the dynamically amplified wind load and the associated BBM.

According to Eq. (8), the displacement is inversely proportional to the first MGM. On the other hand, the BBM in Eq. (10) is not a function of the first MGM or MMI, but is only indirectly affected by the mass by way of the natural frequency. This implies that an increase in mass bears no influence on the BBM response provided that the structural frequency remains the same. In light of this, Bienkiewicz et al. (1986) and Boggs (1991) suggested alternatives to the requirements imposed on mass and associated quantities. For example, if the model can be designed to have the correct mass as required by the preceding scaling laws, then the displacement response will obey the length scale or "100% aeroelastic." It is also possible to design a model which is heavier by a factor of 2 so that the displacement or rotation will be less-than-scale or "50% aeroelastic" or "subaeroelastic;" or on the contrary, a lighter model with larger-than-scale displacement and rotation or "superaeroelastic." In all these cases, although the displacement or rotation may be influenced by the manner in which mass is modeled, the BBM remains the same.

Although the above concept offers a dramatic advantage for aeroelastic model design since the mass similarity ceases to be a requirement, caution must be exercised when modeling the aeroelastic effects. According to the limited available investigations concerning the aeroelastic effects, the mass has been observed to be one of the most pertinent parameters. In fact, the Scruton number, which is proportional to the product of the building air mass ratio and the critical damping ratio, has been recognized to play a key role in the aeroelastic effects (among others, Cheng 1984, Boggs 1991, 1992; CEN 1995). Despite the fact that it may have no effect on the modeling of the aerodynamic forces, an imperfect modeling of mass may result in inaccurate modeling of the aeroelastic effects.

Nonetheless, the available literature provides insufficient guidance on the role of the total mass and the first MGM in modeling aeroelastic effects. The first MGM is usually a small part of the overall mass and could be significantly different depending on the overall mass distribution and the mode shape. Assuming a linear mass distribution

$$m(z) = m_0(1 - \lambda(z/H)) \quad (11)$$

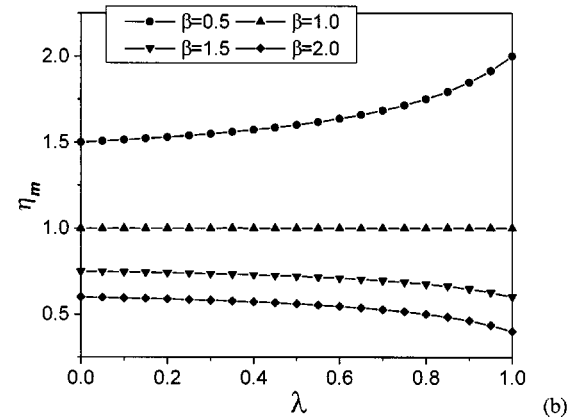
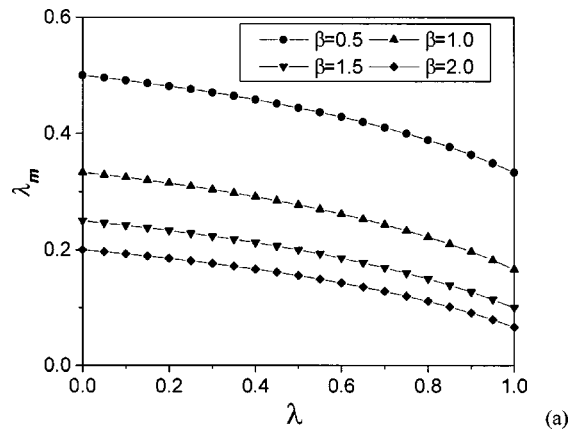


**Fig. 3.** Effects of mode shape on first MGM: (a) ratio to total mass in Eq. (12); (b) ratio to linear first MGM in Eq. (17)

a mass participation factor, which is defined as the ratio between the first MGM to the total mass of the building is given by

$$\lambda_m = \frac{\mathbf{m}}{\mathbf{m}_T} = \frac{2 \cdot [(2 + 2\beta) - \lambda(1 + 2\beta)]}{(2 - \lambda)(2 + 2\beta)(1 + 2\beta)} \quad (12)$$

where  $\lambda = (m_0 - m_H)/m_0$  = mass reduction factor (Boggs and Peterka 1989). Fig. 3(a) shows the sensitivity of  $\lambda_m$  with respect to changes in other parameters. For a uniform mass distribution and a linear mode shape,  $\lambda_m = 0.33$ , or one third of the total mass. It is obvious that the first MGM is sensitive to the distribution of mass and the mode shape. Further study is still called for to clarify the precise roles of the total mass and the first MGM in the aeroelastic modeling of tall buildings.

### Dynamic Similitude: Arbitrary Mode Shape

When the mode shape of a building deviates from a straight line, the similarity between the model and the prototype is not so obvious. A "virtual" building with a linear mode shape is introduced here to build a relationship between the model and the prototype. The virtual building has a linear mode shape and replicates other parameters of the prototype. Since this virtual building has a linear mode shape, its similarity to the model is governed by the scaling laws in the preceding section, while the relationship between the virtual building and the prototype can be expressed through mode shape corrections. Accordingly, the prototype response can be obtained through the virtual building in combina-

tion with a mode shape correction. A detailed discussion of the mode shape corrections has been provided by the writers (Zhou et al. 2002). Some of the relevant relationships for the aeroelastic model testing are described below.

Using the spectral analysis, the displacement response in Eq. (1) is given by

$$\sigma_Y(z) = \frac{1}{(2\pi f_1)^2 \cdot \int_0^H m(z)(z/H)^{2\beta} dz} \cdot \left( \int_0^\infty |H(f)|^2 \cdot S_{p^*}(f) \cdot df \right)^{1/2} \cdot \left( \frac{z}{H} \right)^\beta \quad (13)$$

where  $S_{p^*}(f) = \int_0^H \int_0^H P(z_1, f) P^*(z_2, f) (z_1/H)^\beta (z_2/H)^\beta dz_1 dz_2$  = PSD of the generalized wind force in the first mode; and  $P(z_1, f) P^*(z_2, f)$  = coherence of the externally applied wind pressures.

Using Eq. (37), the first MGM of the model is scaled to the prototype by

$$\mathbf{m}'_m = K_L^3 \cdot K_{\rho_a} \cdot \mathbf{m}_p \quad (14)$$

which is equivalent to a MMI scale as

$$I_m = K_L^5 \cdot K_{\rho_a} \cdot \mathbf{m}_p \cdot H_p^2 \quad (15)$$

The difference between this MMI and that determined by the scale in Eq. (7) can be described by a mode shape effect factor for the first MGM

$$\eta_m = \frac{\int_0^H m(z)(z/H)^{2\beta} dz}{\int_0^H m(z)(z/H)^2 dz} = \frac{12 \cdot [(2+2\beta) - \lambda(1+2\beta)]}{(4-3\lambda)(2+2\beta)(1+2\beta)} \quad (16)$$

This factor is plotted in Fig. 3(b). It can be seen that  $\eta_m$  is sensitive to the mode shape while relatively insensitive to the mass distribution for  $\lambda < 0.5$ . When the mode shape of the building is linear, the factor is, as expected, equal to unity, which indicates the equivalence between the first MGM scale in Eq. (37) and the MMI scale in Eq. (7). However, when the mode shape deviates from a straight line, this equivalence is no longer valid. For  $\beta > 1$ , which may be of concern in most tall building applications,  $\eta_m$  is usually less than unity. For example, when  $\beta = 1.5$ , for a uniform mass distribution,  $\eta_m = 0.75$ , indicating that the use of the MMI scale in Eq. (7) may lead to 33% higher displacement response than that based on the first MGM scale as shown in Eq. (13).

With an accurate modeling of the first MGM in Eq. (14) or MMI in Eq. (15), the displacement response of the virtual building can be computed by

$$\sigma''_Y(z) = \frac{1}{(2\pi f_1)^2 \cdot \int_0^H m(z)(z/H)^{2\beta} dz} \cdot \left( \int_0^\infty |H(f)|^2 \cdot S_M(f)/H^2 \cdot df \right)^{1/2} \cdot \left( \frac{z}{H} \right) \quad (17)$$

where the double prime stands for the virtual building. By comparing Eq. (17) to Eq. (13), the displacement at the virtual building top can be related to the actual displacement by

$$\eta_Y = \left( \frac{\int_0^\infty P(z_1, f) P^*(z_2, f) (z_1/H)^\beta (z_2/H)^\beta df}{\int_0^\infty S_M(f)/H^2 \cdot df} \right)^{1/2} \quad (18)$$

The correction in Eq. (18) is exactly that for the generalized wind force discussed in the literature (e.g., Xu and Kwok 1993; Kijewski and Kareem 1998; Zhou et al. 2002). According to Eq. (18), this factor is a function of the mode shape and the stochastic structure of wind pressure fluctuations. Assuming that the wind

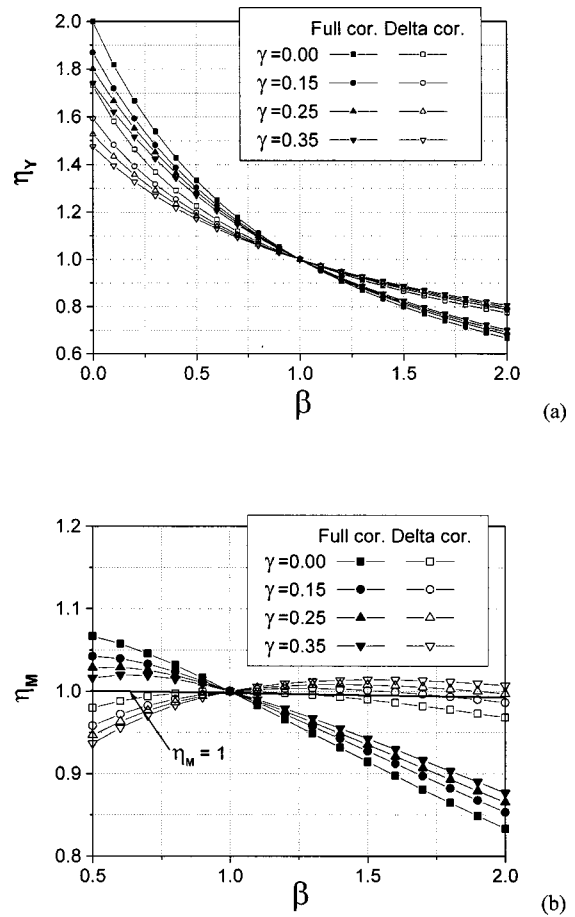


Fig. 4. Mode shape corrections (Zhou et al. 2000): (a) generalized wind load; (b) base bending moment

pressures, including both the aerodynamic and aeroelastic effects, on the building surfaces can be approximately expressed in the following form:

$$P(z_1, f) P^*(z_2, f) = P(z_1) P(z_2) S_p(f) Q(z_1, z_2, f) \quad (19)$$

where  $S_p(f)$  = unit fluctuating wind force spectrum;  $P(z) = P_H(z/H)^\gamma$  in which  $P_H$  = amplitude of the fluctuating wind force evaluated at the building top;  $\gamma$  = fluctuating wind profile exponent; and  $Q(z_1, z_2, f) = \exp(-C_K f / \bar{V} \cdot |z_1 - z_2|/H)$  = correlation of the fluctuating wind pressures in which  $\bar{V}$  = reference wind velocity, and  $C_K$  = exponential decay coefficient. For the fully correlated case  $C_K = 0$  and for delta-correlated case  $C_K \rightarrow \infty$ . It is noted that the structure of the fluctuating wind pressures is related to complicated fluid-structure interactions, and the involved wind pressure parameters may vary significantly for different cases and are seldom available for a particular application unless specifically measured. As reported, the correction factor in Eq. (18) is sensitive to the mode shape, wind exponent, and correlation as shown in Fig. 4(a) (Zhou et al. 2002). In engineering practice, it is usually inconvenient to apply this type of correction since the information on the involved parameters either is not available or can only be approximately determined.

On the other hand, focusing on the BBM response, one can have the following relationship between the virtual and the actual buildings:

$$\sigma_M = \eta_M \cdot \sigma'_M \quad (20)$$

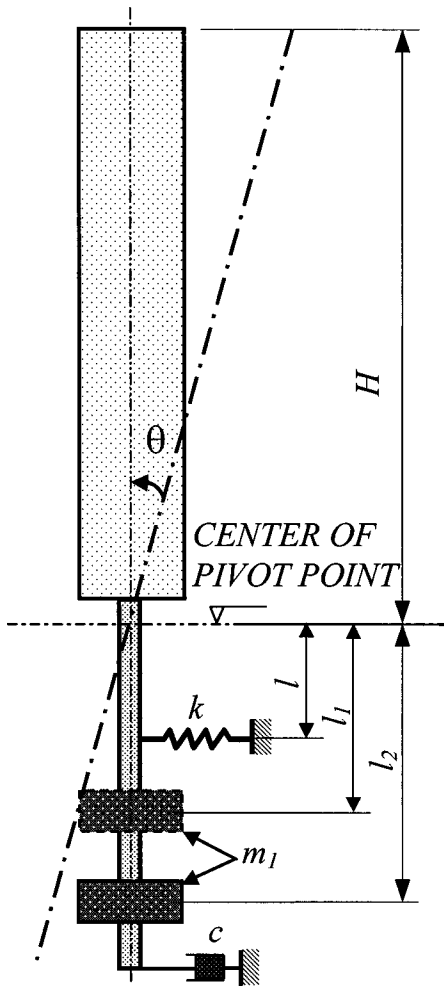


Fig. 5. Model tuning of mass moment of inertia

where  $\eta_M$  = mode shape correction factor for the BBM response; and  $\sigma_M$  and  $\sigma'_M$  = RMS BBM response of the actual building and the virtual building, respectively. As discussed by Zhou et al. (2002),  $\eta_M$  is equal to unity for the background component. For the resonant component, Fig. 4(b) shows the sensitivity of this factor with respect to the involved parameters. It can be seen that for most of the parameter range this factor can be approximately taken as unity without introducing a sizeable error. A similar observation concerning the mode shape correction for the BBM has also been reported by Boggs and Peterka (1989) and AS1170.2-89 (Australian Standards 1989).

### Application of Aeroelastic Balance to Building Design

Based on the preceding scaling relationships, the model can be set up and the measurements on the model can be scaled to the prototype. A detailed description of the model design and model tuning is provided in Appendix II (see Fig. 5).

Ideally, when the mode shape of the prototype building is linear and the mass distribution of the model is the same as that of the prototype, direct similarities between the model and the prototype in terms of displacement, acceleration, or BBM exist. However, these requirements are seldom satisfied in practice. Due to the mismatch in the mode shape and mass distribution between

the model and the prototype, the aeroelastic model test may not provide reliable estimates of building displacement and acceleration response. Furthermore, there are also difficulties in utilizing the displacement and acceleration information obtained from the wind tunnel tests. For example, acceleration measurements reflect only the resonant component contribution, while the displacement measurements are relatively inconvenient, unless the laser-based displacement sensors are employed. On the other hand, the BBM response of an aeroelastic model usually exhibits less sensitivity to the variations in mode shape, mass distribution, and wind pressure parameters. It can also be conveniently measured using regular strain gauges, including the mean, background, and resonant components.

These observations favor an analysis procedure that is based on the BBM measured from the aeroelastic model tests. Drawing a parallel between the BBM by the HFBB and the stick type aeroelastic model, in this paper the latter is called "aeroelastic balance." It is important to note that the BBM measured from the aeroelastic balance is different from that of the HFBB. The former includes the aerodynamic force and aeroelastic feedback, as well as the magnification due to structural dynamics. Besides the insensitivity of the BBM response to the mass and mode shape variations, advantages derived from the BBM-based procedure include the convenient utilization of this information to obtain other quantities of interest, e.g., the ESWL and other wind load effects.

The measured BBM can be expressed in terms of the following nondimensional form that applies to both the model and the prototype structure:

$$C_M(t) = \mathbf{M}(t) / (1/2\rho \bar{V}_H^2 \sqrt{BDH^2}) \quad (21)$$

Accordingly, the ESWL components on the actual building can be computed by (Zhou and Kareem 2001)

$$\bar{\mathbf{P}}(z) = \bar{C}_M \cdot (1/2\rho \bar{V}_H^2 \sqrt{BDH^2}) \left( \frac{2+2\alpha}{H^2} \right) \left( \frac{z}{H} \right)^{2\alpha} \quad (22)$$

$$\sigma_{P_B}(z) = \left( \int_0^{f_1-\epsilon} C_M(f) df \right)^2 \cdot (1/2\rho \bar{V}_H^2 \sqrt{BDH^2}) \left( \frac{2+2\alpha}{H^2} \right) \left( \frac{z}{H} \right)^{2\alpha} \quad (23)$$

$$\sigma_{P_R}(z) = \left( \int_{f_1-\epsilon}^{f_1+\epsilon} C_M(f) df \right)^2 \cdot (1/2\rho \bar{V}_H^2 \sqrt{BDH^2}) \frac{m(z)\varphi(z)}{\int_0^H m(z)\varphi(z)z dz} \quad (24)$$

where  $\bar{\mathbf{P}}$ ,  $\sigma_{P_B}$ , and  $\sigma_{P_R}$  = mean, RMS background and resonant components of the ESWL, respectively;  $\bar{C}_M$  = mean BBM coefficient;  $C_M(f)$  = PSD of the BBM coefficient; and  $\epsilon$  can usually be taken as a tenth of  $f_1$ . For the cases in which the background response is relatively insignificant, Eqs. (23) and (24) can be treated together as the fluctuating component of the ESWL

$$\sigma_{\tilde{P}}(z) = \sigma_{C_M} \cdot (1/2\rho \bar{V}_H^2 \sqrt{BDH^2}) \frac{m(z)\varphi(z)}{\int_0^H m(z)\varphi(z)z dz} \quad (25)$$

where  $\sigma_{\tilde{P}}$  = RMS fluctuating ESWL, including both background and resonant components.

With the ESWL, the wind load effects of interest can be determined by using the above load components with a simple static structural analysis. The resultant response can be combined by a square root of the sum of the squares rule

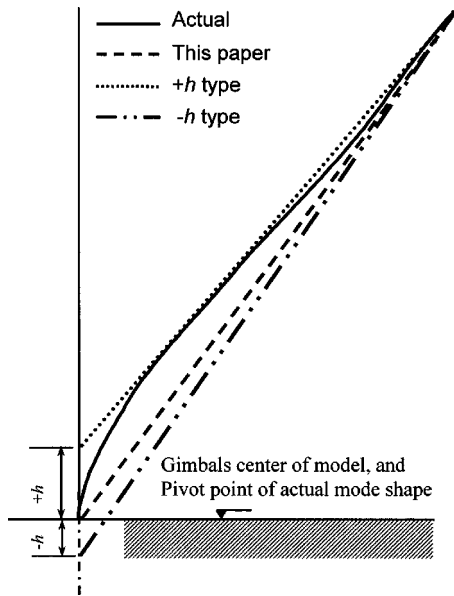


Fig. 6. Mode shape modeling in typical aeroelastic model tests

$$\hat{r} = \bar{r} + g \sqrt{r_B^2 + r_R^2} \quad (26)$$

where  $\hat{r}$ ,  $\bar{r}$ ,  $r_B$ , and  $r_R$  = resultant, mean, background, and resonant response components, respectively;  $g$  = peak factor, which can be determined from statistical analysis of the measured BBM time series or from theoretical consideration (e.g., Davenport 1964) as  $g = \sqrt{2 \ln(f_1 T) + 0.5772 / \sqrt{2 \ln(f_1 T)}}$ , in which  $T$  = observation time.

The displacement and acceleration response can be computed conveniently by

$$Y(z) = \frac{\int_0^H \mathbf{P}(z) \varphi(z) dz}{(2\pi f_1)^2 \cdot \int_0^H m(z) \varphi^2(z) dz} \cdot \varphi(z) \quad (27)$$

$$\sigma_{\ddot{Y}}(z) = \frac{\int_0^H \sigma_{PR}(z) \varphi(z) dz}{\int_0^H m(z) \varphi^2(z) dz} \cdot \varphi(z) \quad (28)$$

where Eq. (27) is applicable to both the mean and the fluctuating components, while Eq. (28) includes only the resonant component.

### Effectiveness of Currently Used Approaches

This section addresses currently used techniques of stick type aeroelastic model tests. One of the approaches is referred to as the “+h type” (Isyumov 1982; Ho et al. 1994), which has also been recommended in ASCE (1999). Another is referred to here as “-h type” (Kareem and Cermak 1978; Boggs 1991). Details of these models are omitted here for the sake of brevity. Fig. 6 schematically compares the modeled mode shapes represented in these model configurations in comparison with the actual building mode shape and the proposal offered in this study. The aim of the +h type model is to “provide the best fit for ... (mode shape) estimations” by adjusting the pivot point to a +h height about the ground (Isyumov 1982); while the -h type model is due to the inherent model setup that renders the pivot point below the wind tunnel floor.

In practice, these models differ in their modeling of the total mass, first MGM, and MMI. For example, for the +h type model,

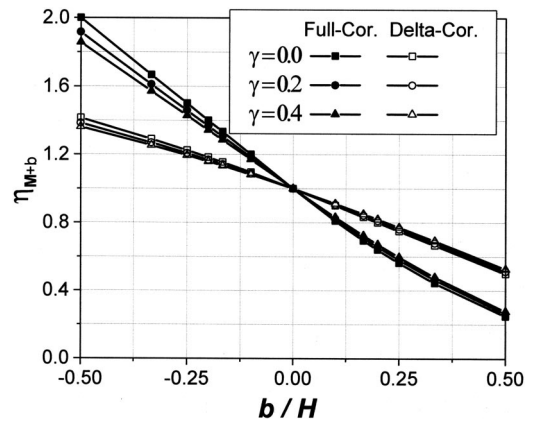


Fig. 7. Effects of deviations of pivot center on measured moments

the computation of the first MGM may entail the integration from either the ground level or from the location defined by +h; and the mode shape may be based on the mode shape of either the prototype or the model. These variations will result in different levels of accuracy in modeling the wind-induced response. Based on the relationship between the externally applied BBM and induced BBM response in Eqs. (10) and (20), the following expression holds for both models:

$$S_{M+b}(f) = |H(f)|^2 \cdot S_{M+b}(f) \quad (29)$$

where subscript  $b$  = distance of the model pivot point from the origin of the actual mode shape, which is +h or -h for the two cases discussed, respectively. Even by ignoring the differences in the modeling of the aeroelastic effects, the BBM response in these two models has the following relationship to that proposed in this paper:

$$\eta_{M+b} = \sigma_{M+b} / \sigma_{M0} \quad (30)$$

in which  $\sigma_{M+b}$  = RMS aerodynamic BBM with regard to the pivot height at +h or -h; and  $\sigma_{M0}$  = RMS aerodynamic BBM with respect to the building base. Fig. 7 shows the variations of  $\eta_{M+b}$  in terms of the wind parameters and the departure of the pivot point from the building base. It can be seen that this factor is insensitive to the wind exponent, but relatively sensitive to the correlation of the pressure field. The information of wind pressure field is normally unavailable, thus making it difficult to use  $\eta_{M+b}$  as correction factors to relate the BBM in the two models discussed to the actual BBM. Furthermore, using a full correlation of aerodynamic pressure field as an example, the BBM is about 70% of the actual value when  $h/H = 1/6$  for the +h type model. Evidently, the farther the pivot point is located from the base, the less the overall wind pressure information is included. On the other hand, the factor is about 1.35 for the same distance of the pivot point in the -h type model.

### Concluding Remarks

This paper examined in detail the role of the aeroelastic balance as a tool for the design of tall buildings. Model scaling laws were derived and their significance in modeling structural dynamics and aeroelastic effects was highlighted. Although the modeling of the building total mass, first MGM, and MMI was treated indiscriminately in most of the current practice, inasmuch as the mass distribution of a prototype building can seldom be precisely reproduced in a small-scale model test, the similarity of the total

mass or the ratio of the structural bulk density to the air density may not adequately ensure the scaling of the first MGM. For buildings with linear mode shapes, it is noted that the correct similarity of the first MGM or MMI is important to ensure accurate aeroelastic modeling.

Many actual tall buildings do not have straight-line mode shapes. On the one hand, the scaling of MMI is usually significantly different from that of the first MGM, while on the other hand, even with accurate modeling of the first MGM the dynamic similarity in the displacement and acceleration response is violated when the prototype building has a nonlinear mode shape. It is shown here that the BBM response measurements exhibit a low sensitivity to the variations in the mass and mode shape. This feature offers an attractive avenue for utilizing the aeroelastic model test in actual design practice through the BBM measurements. The paper provided an analysis procedure for the ESWL and other wind-induced response components derived from the BBM measurements of the aeroelastic balance tests. The efficacy of two currently used aeroelastic modeling approaches is also addressed.

## Appendix I: Derivation of Scaling Laws

This Appendix provides the scaling laws governing the similarities between a tall building with linear mode shape and a stick type aeroelastic model.

Eq. (3) is applicable to both the model and the prototype. For the prototype, it is

$$\begin{aligned} & \ddot{\mathbf{Y}}'_p(t_p) + 4\pi f_{1p}\zeta_p \dot{\mathbf{Y}}'_p(t_p) + (2\pi f_{1p})^2 \mathbf{Y}'_p(t_p) \\ &= \frac{C_{Mp}(t_p, \mathbf{Y}_p, \dot{\mathbf{Y}}_p, \ddot{\mathbf{Y}}_p \dots) \cdot (1/2\rho_{ap}\bar{V}_{pH}^2\sqrt{B_p D_p H_p})}{\mathbf{m}'_p} \end{aligned} \quad (31)$$

where  $\mathbf{Y} = Y_H$ . With an intrinsic linear mode shape, this quantity can be easily related to the displacement at any other height or the rotation angle. For the model, it is

$$\begin{aligned} & \ddot{\mathbf{Y}}'_m(t_m) + 4\pi f_{1m}\zeta_m \dot{\mathbf{Y}}'_m(t_m) + (2\pi f_{1m})^2 \mathbf{Y}'_m(t_m) \\ &= \frac{C_{Mm}(t_m, \mathbf{Y}_m, \dot{\mathbf{Y}}_m, \ddot{\mathbf{Y}}_m \dots) \cdot (1/2\rho_{am}\bar{V}_{mH}^2\sqrt{B_m D_m H_m})}{\mathbf{m}'_m} \end{aligned} \quad (32)$$

If the following similarities exist between the model and the prototype:

$$K_L = \frac{Y_m}{Y_p} = \frac{B_m}{B_p} = \frac{D_m}{D_p} = \frac{H_m}{H_p}, \quad K_V = \frac{V_m}{V_p}, \quad K_t = \frac{t_m}{t_p} = \frac{f_{1p}}{f_{1m}} \quad (33)$$

$$K_{CM} = \frac{C_{Mm}}{C_{Mp}}, \quad K_{\rho_a} = \frac{\rho_{am}}{\rho_{ap}}, \quad K_{m'} = \frac{\mathbf{m}'_m}{\mathbf{m}'_p}, \quad K_{\zeta} = \frac{\zeta_m}{\zeta_p}$$

then Eq. (31) can be recast as

$$\begin{aligned} & \ddot{\mathbf{Y}}'_m(t_m) + \frac{1}{K_{\zeta}} \cdot 4\pi f_{1m}\zeta_m \dot{\mathbf{Y}}'_m(t_m) + (2\pi f_{1m})^2 \mathbf{Y}'_m(t_m) \\ &= \frac{M_m(t_m, \mathbf{Y}_m, \dot{\mathbf{Y}}_m, \ddot{\mathbf{Y}}_m \dots)/H_m}{\mathbf{m}'_m} \\ & \cdot \left( \frac{1}{K_{CM}} \right) \cdot \left( \frac{1}{K_{\rho_a}} \cdot \frac{K_{m'}}{K_L^3} \right) \cdot \left( \frac{K_L}{K_t \cdot K_V} \right)^2 \end{aligned} \quad (34)$$

Comparing Eq. (34) to Eq. (32), the scales in Eq. (33) are ensured by the following conditions:

$$K_{\zeta} = 1 \quad (35)$$

$$K_{CM} = 1 \quad (36)$$

$$K_{m'} = K_L^3 \cdot K_{\rho_a} \quad (37)$$

$$K_L = K_t \cdot K_V \quad (38)$$

Eq. (35) indicates that the damping ratio of the model is the same as that of the prototype. The use of imperfect modeling of damping should be made carefully, since the damping may control the level of aeroelastic effects.

Eq. (36) requires the similarity of the aerodynamic force coefficient. For the aeroelastic model, it includes both aerodynamic forces and aeroelastic feedbacks. The similarity of the aerodynamic force can be ensured by simulating properly the approaching flow, the building surroundings, and the building geometry, which are also required in the HFBB or the pressure model tests. Although these features are sufficient for the aerodynamic tests, the similarity of aeroelastic feedbacks cannot be automatically ensured and it needs additional consideration. There are a number of factors, such as the dimensionless displacement response (Kwok and Melbourne 1981), the reduced wind velocity (Kareem 1982; Tschanz and Davenport 1983), and more recently, Scruton no. (Boggs 1992; CEN 1995), have been reported to be important to the aeroelastic effects. Since the influence of violating scaling laws is not fully understood, it has been suggested that the model should correctly simulate the dynamic characteristics of the structures, including the stiffness, mass, and damping, which influence the aeroelastic effects (ASCE 1999).

Eq. (37) is the scale of the first MGM, which is detailed in the context. Eq. (38) is the scale of the stiffness. For a particular mode that the model simulates, it can also be expressed by

$$(L \cdot f_1 / \bar{V})_p = (L \cdot f_1 / \bar{V})_m \quad (39)$$

which is explained as the reduced frequency or velocity scale, where  $L$  = building dimension. A significant implication of Eq. (39) is that there is no unique requirement concerning the velocity scale, which is inversely proportional to the frequency scale when the length scale is selected. This means the velocity and the frequency scales can be adjusted according to the capability and availability of the wind tunnel facilities. The stiffness modeling can be automatically ensured by correctly simulating the mass and frequency. For some tuning schemes that need accurate stiffness of the model, the scale in Eq. (38) can also be rewritten as

$$K_k = K_{\rho_a} \cdot K_L^5 / K_t^2 \quad (40)$$

By satisfying the above scaling laws, the model will represent a direct similarity with the prototype. In this case, the measurements can be based either on the BBM or the displacement or acceleration at any height or both of them. The model displacement is related to the prototype through the length scale. The acceleration and moment can be scaled to the prototype by

$$K_{\ddot{y}} = K_L / K_t^2 \quad (41)$$

$$K_M = K_{\rho_a} \cdot K_L^5 / K_t^2 \quad (42)$$

For the case of a building with exactly a linear mode shape, there exists a crosscheck between the displacement and the BBM measurements. The ESWL on the actual building can be determined based on the information of either of them. General pro-

cedures based on the BBM information are provided in the context and the procedure for the building with a linear mode shape can be treated as a special case.

## Appendix II: Model Design and Calibration

### Prototype Information

The information of the prototype that is necessary for model design includes the first MGM, total mass, interested wind velocity range, damping ratio, and frequency in the first two sway modes.

### Model Scales

The length scale needs to be selected at first, which should consider the wind tunnel blockage, the modeled turbulence length scale, and constraints on model construction, e.g., the mass requirement. Once selected, the model as well as the ambient structures and their locations need to be built in the same scale. After the selection of length scale, the wind velocity scale and the frequency scale can be intentionally adjusted to fit the capability of the wind tunnel facilities. The air density scale is fixed and usually very close to unity. Special attention needs to be paid when there is a significant difference between the model and the prototype in temperature or elevation.

### Model Tuning

Install the model following the setup as shown in Fig. 1(a). Align the pivot center of the model to the corresponding height of the origin of the actual mode shape. Adjust the damping ratio of the model system to the accurate values as those used in the structural analysis for the prototype building. These values can vary according to the consideration of a different limit state of design.

The mass of the model can then be determined after the air density and length scales have been selected by using Eq. (6). The total mass budget includes all the components that participate in the vibration, such as the building model, spring, supporting rods, tuning mass, transducer, etc. It is noted that this modeling requirement for total mass is not discarded until sufficient data are available to show that its role in the modeling of aeroelastic effects is insignificant.

The first MGM of the model can be determined using Eq. (15). However, since it is usually inconvenient to directly measure the first MGM of the model; one alternative is to adjust the MMI of the model based on Eq. (16). The accurate value of the MMI of the model can be determined through a tuning mass by

$$I_{l_2} = m_1 \cdot (\Delta l^2 + 2 \cdot l_1 \cdot \Delta l) \cdot (f_{l_1}^2 / (f_{l_1}^2 - f_{l_2}^2)) \quad (43)$$

in which  $l_1$ ,  $l_2$ , and  $m_1$  are shown in Fig. 5;  $f_{l_1}$  and  $f_{l_2}$  denote the frequencies when the tuning mass is placed at heights  $l_1$  and  $l_2$  below the pivot point, respectively; and  $\Delta l = l_2 - l_1$ . Another alternative is to determine the target stiffness of the model first using the scale in Eq. (40) and then tune the first MGM to the targeted frequency.

### Imperfect Modeling

For many actual buildings with different mode shapes in two lateral directions, the first MGM in each direction may be different. Since the model has linear mode shape in each direction, it is

not possible to have different first MGM in each direction. In this situation, an imperfect modeling is considered by determining the first MGM of the model as

$$\mathbf{m}'_m = (K_L^3 \cdot K_{\rho_a})^{1/2} (\mathbf{m}_{pX} + \mathbf{m}_{pY}) \quad (44)$$

For many actual buildings the frequencies in two directions may be different from each other. The ratio of the frequencies (Cermak 1977) needs to be modeled by adjusting the target frequencies through tuning the stiffness in the two directions

$$(f_X / f_Y)_m = (f_X / f_Y)_p \quad (45)$$

## References

- American Society of Structural Engineers. (ASCE). (1999). *ASCE manuals and reports on engineering practice No. 67. Wind tunnel studies of buildings and structures*, ASCE, Reston, Va., 20191–4400.
- Australian Standards. (1989). “SAA Loading code, part 2—wind forces.” *AS1170.2-89*, Australia.
- Bienkiewicz, B., Cermak, J. E., and Peterka, J. A. (1986). “Scaling of building models for wind tunnel tests.” *Advancements in aerodynamics, fluid mechanics and hydraulics*, R. E. A. Arndt et al., eds., ASCE, New York, 806–813.
- Boggs, D. W. (1991). “Wind loading and response of tall structures using aerodynamic models.” PhD dissertation, Colorado State Univ., Fort Collins, Colo.
- Boggs, D. W. (1992). “Validation of the aerodynamic model method.” *J. Wind. Eng. Ind. Aerodyn.*, 41–44, 1011–1022.
- Boggs, D. W., and Peterka, J. A. (1989). “Aerodynamic model tests of tall buildings.” *J. Eng. Mech.*, 115(3), 618–635.
- Cermak, J. E. (1977). “Wind-tunnel testing of structures.” *J. Eng. Mech. Div., Am. Soc. Civ. Eng.*, 103(6), 1125–1140.
- Cheng, C. M. (1984). “Across-wind response of towers and stacks of circular cross-section.” PhD dissertation, Univ. of Houston, Houston.
- Davenport, A. G. (1964). “Note on the distribution of the largest value of a random function with application to gust loading.” *Proc., Institution of Civil Engineers*, London, 28, 187–196.
- European Committee for Standardization (CEN). (1995). “Basis of design and actions on structures—Part 2–4: Actions on structures—Wind actions.” *Eurocode 1, European Prestandard ENV 1991-2-4*.
- Gu, M., Zhou, Y., Zhang, F., and Xiang, H. F. (1999). “Determining wind loads on Jinmao Building.” *Proc., 10th Int. Conf. on Wind Engineering*, Copenhagen, Denmark, 1497–1504.
- Ho, T. C. E., Isyumov, N., Mikitiuk, M. J., and Crooks, G. J. (1994). “A study of wind effects for the Jin Mao Building project, Shanghai, China—Final report.” *Rep. No. BLWT-SSI-1994*, Univ. of Western Ontario, Ont., Canada.
- Holmes, J. D. (1987). “Mode shape corrections for dynamic response to wind.” *Eng. Struct.*, 9, 210–212.
- Isumov, N. (1982). “The aeroelastic modeling of tall buildings.” *Wind tunnel modeling for civil engineering applications*, Timothy A. Reinhold, ed., 373–407.
- Kareem, A. (1982). “Acrosswind response of buildings.” *J. Struct. Eng.*, 108(4), 869–887.
- Kareem, A. (1984). “Model for predication of the across-wind response of buildings.” *Eng. Struct.*, 6(2), 136–141.
- Kareem, A., and Cermak, J. E. (1979). “Wind-tunnel simulation of wind-structure interactions.” *ISA Trans.*, 18(4), 23–41.
- Kijewski, T., and Kareem, A. (1998). “Dynamic wind effects: A comparative study of provisions in codes and standards with wind tunnel data.” *Wind Struct.*, 1(1), 77–109.
- Kwok, K. C. S., and Melbourne, W. H. (1981). “Wind-induced lock-in excitation of tall structures.” *J. Struct. Div., ASCE*, 107(1), 57–72.

- Langhaar, H. L. (1951). *Dimensional analysis and theory of models*, Wiley, New York.
- Saunders, J. W., and Melbourne, W. H. (1975). "Tall rectangular building response to cross-wind excitation." *Proc., 4th Int. Conf. on Wind Effects on Buildings and Struct.*, Cambridge Univ. Press, Cambridge, U.K., 369–379.
- Tschanz, T., and Davenport, A. G. (1983). "The base balance technique for the determination of dynamic wind loads." *J. Wind. Eng. Ind. Aerodyn.*, 13, 429–439.
- Vickery, B. J. (1970). "On the reliability of gust loading factors." *Proc., Technical Meeting Concerning Wind Loads on Buildings and Structures, Building Science Series 30*, National Bureau of Standards, Washington, D. C., 296–312.
- Vickery, P. J., Steckley, A. C., Isyumov, N., and Vickery, B. J. (1985). "The effect of mode shape on the wind-induced response of tall buildings." *Proc., 5th U.S. Natl. Conf. on Wind Engineering*, Texas Tech. Univ., Lubbock, Tex.
- Whitebread, R. E., and Scruton, C. (1965). "An investigation of the aerodynamic stability of a model of the proposed tower blocks for the World Trade Center, New York." National Physical Laboratory Aero. Rep. No. 1165, England.
- Xu, Y. L., and Kwok, K. C. S. (1993). "Mode shape corrections for wind tunnel tests of tall buildings." *Eng. Struct.*, 15(5), 387–392.
- Zhou, Y., Gu, M., and Xiang, H. F. (1999). "Along-wind static equivalent wind loads and response of tall buildings. Part II: Effects of mode shapes." *J. Wind. Eng. Ind. Aerodyn.*, 79(1–2), 151–158.
- Zhou, Y., and Kareem, A. (2001). "Gust loading factor: New model." *J. Struct. Eng.*, 127(2), 168–175.
- Zhou, Y., Kareem, A., and Gu, M. (2002). "Mode shape corrections for wind load effects." *J. Eng. Mech.*, 128(1), 15–23.